# Wave climate variability in the North Atlantic in recent decades in the winter period using numerical modeling

**Article** *in* Oceanology · May 2016

DOI: 10.1134/S0001437016030140

CITATIONS
5

READS
40

**2 authors**, including:

Alexander Gavrikov
P.P. Shirshov Institute of Oceanology
**47** PUBLICATIONS **225** CITATIONS

SEE PROFILE

ISSN 0001-4370, Oceanology, 2016, Vol. 56, No. 3, pp. 320–325. © Pleiades Publishing, Inc., 2016.
Original Russian Text © M.Yu. Markina, A.V. Gavrikov, 2016, published in Okeanologiya, 2016, Vol. 56, No. 3, pp. 346–352.

MARINE PHYSICS

# Wave Climate Variability in the North Atlantic in Recent Decades in the Winter Period Using Numerical Modeling[1]

**M. Yu. Markina and A. V. Gavrikov**

*Shirshov Institute of Oceanology, Russian Academy of Sciences, Moscow, Russia*

*e-mail: markina@sail.msk.ru, gavr@sail.msk.ru*

Received June 3, 2015; in final form, November 19, 2015

**Abstract**—The study focuses on investigating significant wave height, including both mean and extreme values, in the North Atlantic in winter during the period from 1979 to 2010. We perform a 32-year wind wave hindcast for the North Atlantic using a spectral ocean wave model (WaveWatch III) and a high-resolution nonhydrostatic atmospheric model (WRF-ARW), which provides the wind forcing function. Analysis of the 32-year hindcast of wave characteristics in the North Atlantic reveals stronger mean and extreme waves simulated with high resolution modeling systems and identifies significant downward trends in the mean significant wave height in the subpolar North Atlantic. Such trends were not found in the wave characteristics from ERA-Interim reanalysis. At the same time, the 32-year hindcast did not confirm the statistically significance of strong positive trends in the central Atlantic diagnosed by ERA-Interim reanalysis; differences between the reanalysis and hindcast are discussed.

**DOI:** 10.1134/S0001437016030140

## INTRODUCTION

Reliable information about wind-generated waves and their variability over the North Atlantic region is essential due to the need for accurate wave data in the planning of marine operations and building offshore and coastal structures. At the same time, the North Atlantic is characterized by a relatively large number of highly intensive storms in comparison to other ocean basins [10, 11]. The climatology of wind waves is very important for understanding general climate changes in processes in ocean–atmosphere interaction processes. Wind waves integrate atmospheric characteristics, so they are an important indicator of the state of the lower atmosphere and its interaction with the ocean [12]. Wind waves play an important role in mixing of the upper ocean, so their dynamics and interannual variability also show changes in ocean structure.

To estimate the mean and extreme wave characteristics of the entire ocean basin, it should be covered with high-resolution data. Though there are many different types of wave data in the North Atlantic in comparison with other parts of the World Ocean, the spatial density of these data is insufficient [11] for comprehensive analysis of the wind wave climate, especially the wave dynamics and extreme characteristics. The most effective approach is reconstruction of wave fields using numerical modeling based on the proper boundary conditions, model forcing, and optimal configuration of experiments.

[1] The article was translated by the authors.

Much research has been devoted to numerical wave modeling of the North Atlantic Basin with the objective of obtaining the interannual variability of the wave climate and wave dynamics [9, 14, 22, 26, 27]. This research. However, they consider only relatively small coastal areas, or low spatial resolution and use reanalysis forcing fields in the wave models. Here we use a wave model with a high-resolution grid in conjunction with a high-resolution nonhydrostatic atmospheric model. The spatial domain covers the entire North Atlantic basin from 20° to 70° N and from 80° to 0° W.

## METHODS

### *Wave Model*

The spatial and temporal resolution of the initial (wind) fields is one of the key components that affects the quality of the output fields in wave modeling, because numerical schemes are very sensitive to the resolution and quality of the initial fields. All spectral wave models also have different parametrization schemes that determine such main wave processes as energy input and dissipation, nonlinear wave interactions, depth-induced breaking, wave–bottom interactions, bottom scattering, and interaction with currents and ice. In this study, we use the third-generation spectral wave model WaveWatch (WW3) v. 4.18, which is based on the energy balance equation. It has been actively developed by many research groups, predominately by the United States's National Oceanic and Atmospheric Administration (NOAA). This model is

applicable both for operational use and long-term numerical simulations [23].

In order to choose the most optimal parametrization schemes of the main wave processes, a number of sensitivity tests were run. One of the most important parts of every wave model is the block responsible for energy input and dissipation, so after a number of tests we used the scheme developed by the Babanin group (Babanin, Young, Donelan, Rogers, Zieger) [3–5, 20]). This scheme includes swell dissipation, which is important for numerical simulations in a large area. The parametrized nonlinear wave interaction DIA (discrete interaction approximation) scheme [24] is widely used in practical wave modeling because of its sufficient computational economy. In the present study, we used an evolution of this scheme—GMD (generalized multiple DIA), which is one of the unique features of the latest version of the WaveWatch III model. The wave model was run on a spherical regular grid with a global horizontal resolution of 0.2° (~20–25 km) and a spectral resolution of 40 frequencies and 36 directions, with a global time step 900 s and output records every hour. This configuration is the most optimal balance between the quality of output fields and requirements on computational resources for long-term numerical simulations.

### *Initial and Boundary Conditions*

Conventional atmospheric forcing for wave models comes from reanalysis data; however, they usually have a relatively low spatial resolution. They also tend to be produced by hydrostatic atmospheric models, where geostrophic adjustment dominates over non-geostrophic effects. This prevents the correct description of vertical atmospheric motion. To avoid this effect, we use a regional version of the high-resolution nonhydrostatic atmospheric model Weather Research and Forecasting (WRF) with the Advanced Research core [21, 25] to produce the initial wind fields for the wave model. Ocean boundaries in the wave model are open, so we neglect swell coming to the southern boundary of the computational domain; this aspect should be considered more carefully in future studies.

In order to choose the number of the most optimal parametrization schemes for grid and subgrid processes, sensitivity tests for the atmospheric model were run as well as for the wave model. The final configuration of the atmospheric model consists of many parts: the MYNN2 scheme for planetary boundary layer parametrization [18]; the Eta model scheme for the surface layer [7]; the CAM scheme for radiation fluxes [8]; an updated Kain–Fritsch scheme for convective processes [15, 16]; the WSM3 scheme for microphysics [13], the Noah land surface model [17]. Boundary conditions for the WRF model were produced by ERA-Interim atmospheric reanalysis. The spatial resolution of the WRF model was 15 km with 30 vertical layers, output every 6 h.

WW3 model and ERA-Interim verification versus NDBC buoys (for significant wave heights)

| Buoy no. | Errors | | |
|---|---|---|---|
| | δ *Hs*, m ERAi/WW3 | α *Hs*, m ERAi/WW3 | ρ *Hs*, % ERAi/WW3 |
| 41002 | 0.43/0.72 | 0.13/0.3 | 20/–11 |
| 41004 | 0.47/0.47 | 0.22/0.25 | –4 /–10 |
| 41010 | 0.35/0.6 | 0.14/0.3 | –5/–16 |
| 44004 | 0.63/1.01 | 0.17/0.31 | –1/–18 |
| 44005 | 0.42/0.74 | 0.15/0.32 | –5/–17 |
| 44007 | 0.72/0.68 | 0.50/0.38 | 17 /–16 |
| 44008 | 0.63/0.98 | 0.17/0.30 | –2/–13 |
| 44009 | 0.59/0.67 | 0.23/0.35 | –12/–10 |
| 44011 | 0.50/0.73 | 0.15/0.28 | –2/–15 |
| 44014 | 0.37/0.74 | 0.16/0.32 | –6/8 |

### *Verification of the Model*

The results of the wave model were verified by comparison with buoys of NOAA National Data Buoy Center (NDBC) [19] and two-dimensional fields from the ERA-Interim wave reanalysis [6], which has the main parameters of the sea state on a 1 degree horizontal resolution grid every 6 h. The table presents the results of comparison of both ERA-Interim wave reanalysis and WW3 model with ten NDBC buoys (for January 2000, time step 6 h).

Figure 1 shows the time series of significant wave height in buoy 44009 according to buoy data, ERA-Interim wave reanalysis, and wave model results for January 2000.

The following errors were computed for reanalysis and model verification [2].

Root mean square error:

$$\delta P = \left( \frac{1}{N_{\text{obs}}} \sum_{n=1}^{N_{\text{obs}}} [P_{\text{num}}(n) - P_{\text{obs}}(n)]^2 \right)^{1/2}. \quad (1)$$

Relative root mean square error:

$$\rho P = \left( \frac{1}{N_{\text{obs}}} \sum_{n=1}^{N_{\text{obs}}} \left( \frac{P_{\text{num}}(n) - P_{\text{obs}}(n)}{P_{\text{obs}}(n)} \right)^2 \right)^{1/2}. \quad (2)$$

Arithmetic error:

$$\alpha P = \left( \frac{1}{N_{\text{obs}}} \sum_{n=1}^{N_{\text{obs}}} (P_{\text{num}}(n) - P_{\text{obs}}(n)) \right). \quad (3)$$

$N_{\text{obs}}$ is the length of the data array of characteristic $P$ (here, it is the significant wave height), $P_{\text{obs}}$ is observed data, and $P_{\text{num}}$ is reanalysis or model output; summation over time.

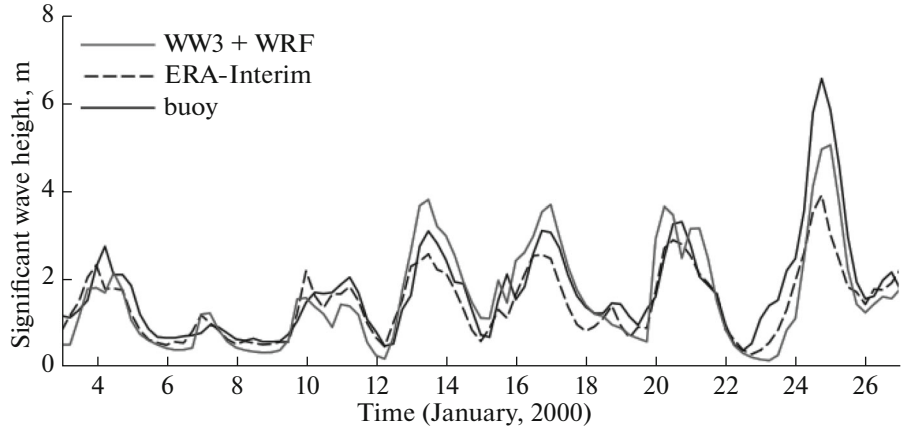


**Fig. 1.** Time series of significant wave height for buoy 44009: reanalysis (ERAi), results of numerical modeling (WW3 + WRF), and buoy data (buoy).

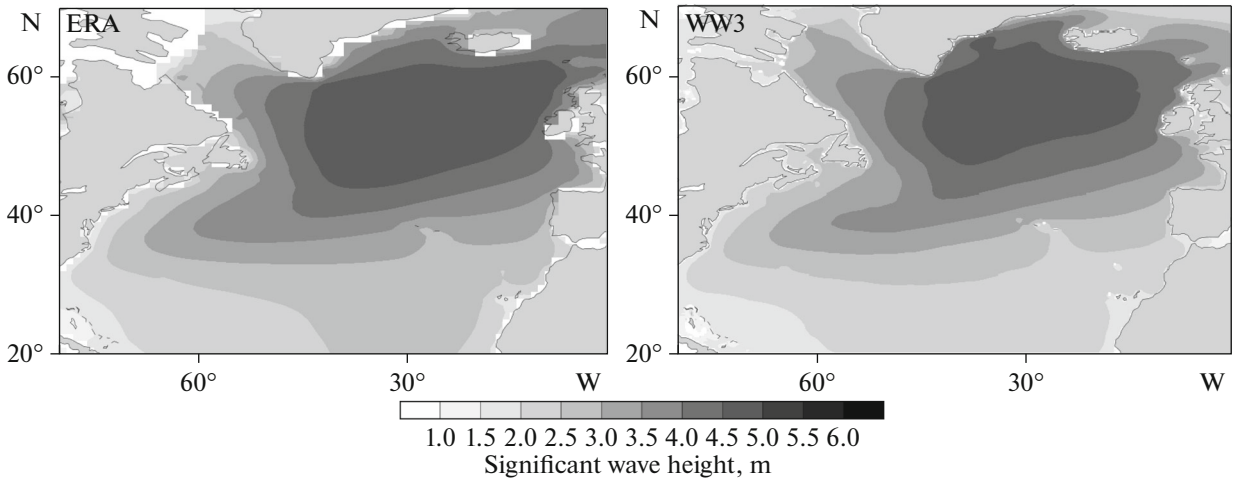


**Fig. 2.** Climate mean significant wave heights at every point in period of 1979–2010 (January).

Observational data are assimilated in the ERA-Interim reanalysis algorithm, so, naturally, matching between buoys and reanalysis is better than the same for the WW3 model. However, general correspondence between buoys and models is acceptable. At the same time, the WW3 resolution makes it possible to resolve structures unavailable for reanalysis and to perform more particular research of extreme characteristics (Fig. 1).

The results of comparison between two-dimensional fields from the ERA-Interim and WW3 model will be discussed below with the main results.

## MAIN RESULTS

Wind wave fields in the North Atlantic for the period from 1979 to 2010 in wintertime were reconstructed using the WW3 model in conjunction with the WRF atmospheric model with a spatial resolution of 0.2° and output every hour. The output data arrays consist of the main wind wave characteristics: significant wave height (including swell), mean wave and peak directions, mean direction of energy transfer, mean absolute and relative wave periods, normalized width of the wave spectrum, and other parameters. For now, we analyzed mean significant wave heights and their interannual variability for every point in the computational domain. The linear trends of these characteristics, including their statistical significance, were estimated.

In general, WW3 waves show good agreement with the ERA-Interim data (Fig. 2). The highest mean significant waves are associated with the Icelandic Low and are about 5 m according to both databases.

Analysis of the spatial distribution of trends in mean significant wave heights also shows good agreement, but the areas of statistical significance (by Student's *t*-test with a significance level of 90%) are quite different (Fig. 3, upper panel; lining is used for areas with statistical significant trends). According to ERA-Interim reanalysis, there is a large area with positive trends in significant wave height (up to 3 cm/yr). WW3 reveals these positive trends too, but they are consid-

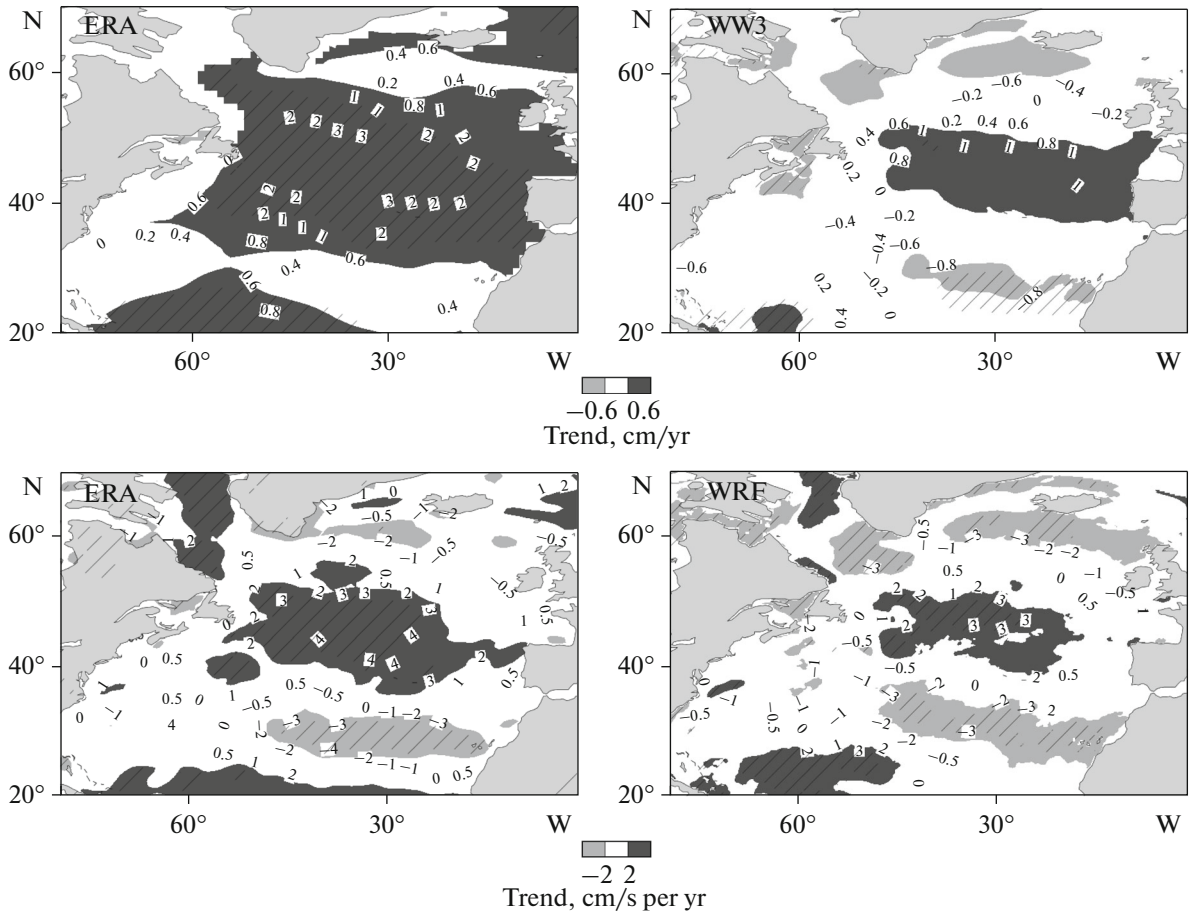


**Fig. 3.** Interannual variability of SWH (upper panel) and 10-m wind speed (lower panel) according to ERA-Interim reanalysis (left side) and WW3 + WRF modeling (right side) in period of 1979–2010 (January); lining is used for area of significant trends.

ered statistically insignificant. However, there are downward trends in the eastern part of the subtropical Atlantic. For both ERA-Interim reanalysis and WRF (which has the ERA-Interim boundary conditions), wind fields show the same areas with positive trends in the middle of the North Atlantic (~3 cm/s per year) and negative in the subtropical region (~3 cm/s per year).

Extreme wave characteristics (we considered waves of the highest tenth percentile to be extreme $Hs_{90}$) at every grid point, and their statistically significant trends were analyzed (Fig. 4).

Maximum extreme waves are 7.1 m for reanalysis and 7.64 m for the WW3 model; the maximum extreme wind speed is 18.9 m/s for the ERA-Interim reanalysis and 22.12 m/s for the WRF model. Despite the fact that the absolute values of mean waves are not that different, the extreme wave fields in the WW3 model (Fig. 4, upper right panel) have a more detailed structure with local areas with extremes near the eastern Greenland coast, which is revealed by the North Atlantic Wave Atlas [1]. In general, extreme waves obtained with the WW3 model are about 10% higher in the subpolar Atlantic than for the reanalysis.

The significant trends of the spatial distribution of extreme waves are inconsistent with the reanalysis (Fig. 4, lower panel), as in the case of the mean characteristics. There is an area with positive trends in the central Atlantic according to the reanalysis (~3 cm/yr). In model experiments with the WRF wind, there is an area with a negative trend (~2 cm/yr) in the Labrador Sea, which is not revealed by the reanalysis. Ice fields were not assimilated into the wave model in the present experiments, so these results should be considered carefully, but at the same time they agree with the study [22].

The regional temporal evolution of anomalies in the occurrence of different significant wave heights were analyzed for the entire period (not presented here). This diagnostic was implemented for the area with positive trends in the central Atlantic (45°–55° N, 40°–50° W). The temporal evolution of anomalies in wind waves has a similar structure for both databases; however, there are significant differences in high waves. There is an increasing number of high waves in 1982, 1990 and 2003, which correlates with the North Atlantic Oscillation (NAO).

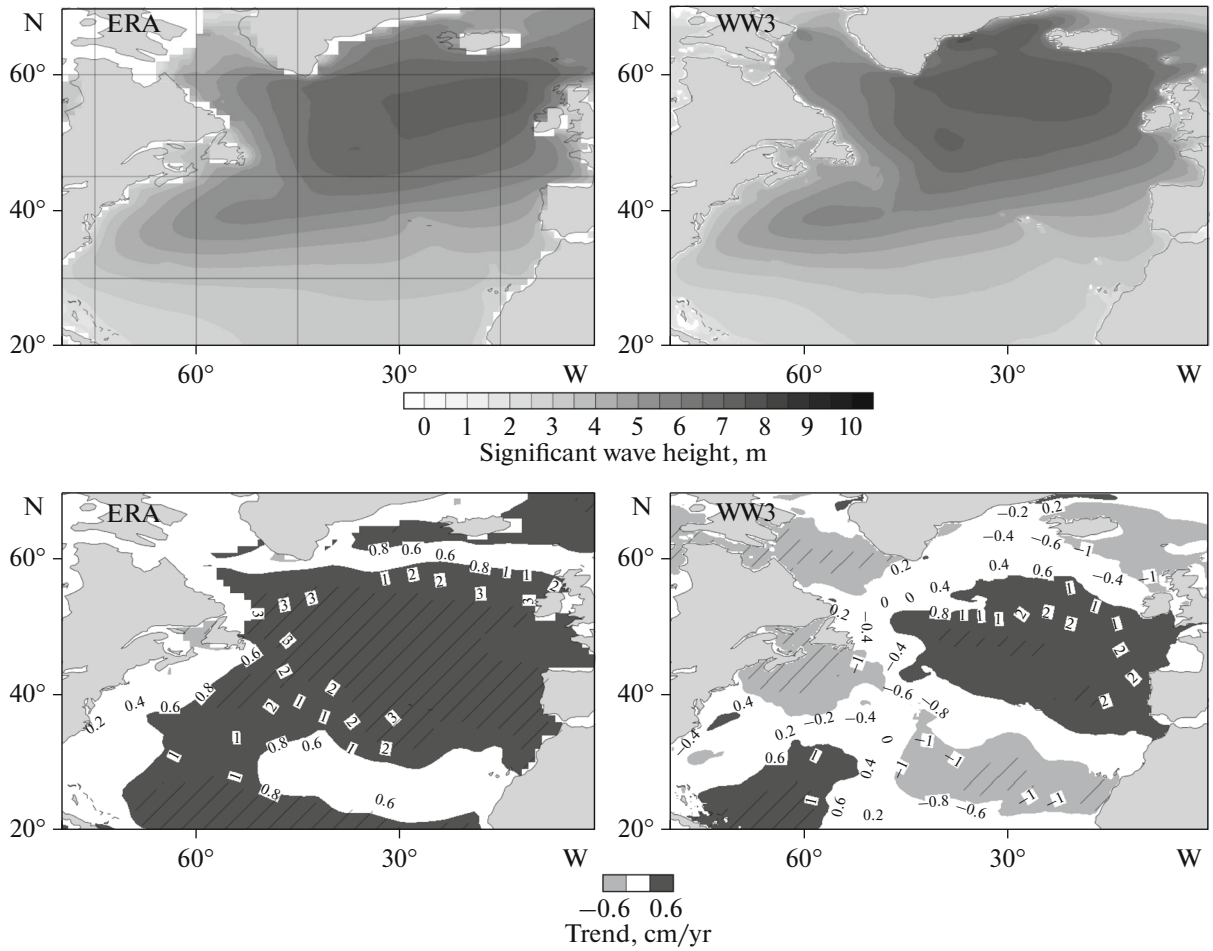


**Fig. 4.** Climate mean upper tenth percentile SWH (upper panel) and its interannual variability (lower panel) according to ERA-Interim wave reanalysis (left) and WW3+WRF modeling (right) in period of 1979–2010 (January); lining is used for area of significant trends.

In summary, a long-term numerical experiment was performed over the North Atlantic region for the last three decades; the output of the hindcast consists of basic wind and wave characteristics. A high-resolution atmospheric model in conjunction with a high resolution-wave model gives the highest extremes of wind and waves (up to 10% in some regions) in the subpolar Atlantic. Interannual variability characteristics revealed by the reanalysis and high-resolution modeling show some inconsistences. In the WW3 model, the results have no significant trends in the central Atlantic, but there is a negative trend in significant wave heights in the subpolar regions to south of Greenland and in the eastern subtropics. Strong negative trends in the Labrador Sea should be analyzed more properly after assimilating ice fields.

## ACKNOWLEDGMENTS

This study was supported by the Russian Science Foundation under contract no. 14-50-00095. Numerical experiments in this study were supported by the Supercomputing Center of Moscow State University and the Joint Supercomputer Center of the Russian Academy of Sciences.

## REFERENCES

1. *Atlas of Waving in the Northern Atlantic* (Artifaks, Obninsk, 2009) [in Russian].
2. V. G. Polnikov, "An extended verification technique for solving problems of numerical modeling of wind waves," Izv. Atmos. Ocean. Phys. **46** (4), 511–523 (2010).
3. A. V. Babanin, "Breaking of ocean surface waves," Acta Phys. Slov. **59**, 305–535 (2011).
4. A. V. Babanin, *Breaking and Dissipation of Ocean Surface Waves* (Cambridge Univ. Press, Cambridge, UK, 2011).
5. A. V. Babanin, M. L. Banner, and I. R. Young, "Breaking probabilities for dominant surface waves on water of finite constant depth," J. Geophys. Res. **106**, 11659–11676 (2001).
6. P. Berrisford, D. Dee, P. Poli, et al., *ERA Report Series: 1. The ERA-Interim Archive, Version 2.0* (European

Centre for Medium-Range Weather Forecasts, Shinfield Park, Reading, UK, 2011).

7. F. Chen, Z. Janjic, and K. Mitchell, "Impact of atmospheric surface layer parameterizations in new land-surface scheme of the NCEP Mesoscale Eta model," Boundary-Layer Meteorol. **3**, 391–421 (1997).
8. W. D. Collins, P. J. Rasch, B. A. Boville, J. J. Hack, J. R. McCaa, D. L. Williamson, J. T. Kiehl, B. Briegleb, C. Bitz, S.-J. Lin, M. Zhang, and Y. Dai, "Description of the NCAR community atmosphere model: CAM3," in *Technical Report NCAR/TN-464+STR* (National Center for Atmospheric Research, Boulder, CO, 2004).
9. G. Dodet, X. Bertin, and R. Taborda, "Wave climate variability in the North-East Atlantic over the last six decades," Ocean Model. **31**, 120–131 (2010).
10. S. K. Gulev and V. Grigorieva, "Variability of the winter wind waves and swell in the North Atlantic and North Pacific as revealed by the voluntary observing ship data," J. Clim. **19**, 5667–5785 (2006).
11. S. Gulev, V. Grigorieva, A. Sterl, and D. Woolf, "Assessment of the reliability of wave observations from voluntary observing ships: Insights from the validation of a global wind wave climatology based on voluntary observing ship data," J. Geophys. Res., C: Oceans Atmos. **108** (7), 3236–3257 (2003).
12. S. K. Gulev and L. Hasse, "North Atlantic wind waves and wind stress from voluntary observing data," J. Phys. Oceanogr. **28**, 1107–1130 (1998).
13. S.-Y. Hong, J. Dudhia, and S.-H. Chen, "A revised approach to ice microphysical processes for the bulk parameterization of clouds and precipitation," Mon. Weather Rev. **132**, 103–120 (2004).
14. C. Izaguirre, M. Menendez, P. Camus, et al., "Exploring the interannual variability of extreme wave climate in the Northeast Atlantic Ocean," Ocean Model. **59–60**, 31–40 (2012).
15. J. S. Kain, "The Kain-Fritsch convective parameterization: an update," J. Appl. Meteorol. **43**, 170–181 (2004).
16. J. S. Kain and J. M. Fritsch, "A one-dimensional entraining detraining plume model and its application in convective parameterization," J. Atmos. Sci. **47**, 2784–2802 (1990).
17. L. Mahrt and H. L. Pan, "A two-layer model of soil hydrology," Boundary-Layer Meteorol. **29**, 1–20 (1984).
18. M. Nakanishi and F. Niino, "Development of an improved turbulence closure model for the atmospheric boundary layer," J. Meteorol. Soc. Jpn. **87** (5), 895–912 (2009).
19. *NDBC Technical Document 09-02, Handbook of Automated Data Quality Control Checks and Procedures* (National Data Buoy Center, Mississippi, 2009).
20. W. E. Rogers, A. V. Babanin, and D. W. Wang, "Observation-consistent input and whitecapping-dissipation in a model for wind-generated surface waves: description and simple calculations," J. Atmos. Ocean. Tech. **29**, 1329–1346 (2012).
21. W. C. Skamarock, J. B. Klemp, J. Dudhia, et al., *A Description of the Advanced Research WRF Version 3, NCAR Technical Note* (National Center for Atmospheric Research, Boulder, CO, 2008).
22. V. R. Swail, E. A. Ceccacci, and A. T. Cox, "The AES40 North Atlantic wave reanalysis: validation and climate assessment," in *6th International Workshop on Wave Hindcasting and Forecasting, November 6–10, 2000* (Monterey, CA, 2000).
23. H. L. Tolman, *User Manual and System Documentation of WAVEWATCH-III Version 3.14, NOAA/NWS/NCEP/MMAB Technical Note 276* (National Weather Service, Camp Springs, MD, 2014).
24. H. L. Tolman, *A Genetic Optimization Package for the Generalized Multiple DIA in WAVEWATCH III, Version 1.4, NOAA/NWS/NCEP/MMAB Technical Note 289* (National Weather Service, Camp Springs, MD, 2014).
25. W. Wang, D. Barker, J. Bray, et al., *User's Guide for Advanced Research WRF (ARW) Modeling System Version 2* (National Center for Atmospheric Research, Boulder, CO, 2008). http://www.mmm.ucar.edu/wrf/users/docs/user_guide_V3/ARWUsersGuideV3.pdf.
26. X. L. Wang, F. W. Zwiers, and V. R. Swail, "North Atlantic Ocean wave climate change scenarios for the twenty-first century," J. Clim. **17**, 2368–2383 (2003).
27. D. K. Woolf and P. G. Challenor, "Variability and predictability of the North Atlantic wave climate," J. Geophys. Res., C: Oceans Atmos. **107** (10), 3145–3159 (2002).